

# Quantum-mechanical tunneling of water in heme proteins

Don C. Lamb,<sup>1</sup> Jan Kriegl,<sup>2</sup> Klaus Kastens<sup>2</sup> and G. Ulrich Nienhaus<sup>1,2\*</sup>

<sup>1</sup>Department of Physics, University of Illinois at Urbana–Champaign, Urbana, Illinois 61801, USA

<sup>2</sup>Department of Biophysics, University of Ulm, D-89069 Ulm, Germany

Received 29 December 1999; revised 7 April 2000; accepted 12 April 2000

**ABSTRACT:** Heme proteins are nanolaboratories that can be used to investigate chemical and biochemical phenomena. For example, the rebinding of carbon monoxide to the Fe<sup>2+</sup>–protoporphyrin-IX prosthetic group in heme proteins after photodissociation at low temperature (<50 K) proceeds predominantly via quantum-mechanical tunneling, as implied by the presence of an isotope effect on the recombination rate coefficients. Heme proteins are among the few systems where the tunneling of entire molecules has been studied in depth. Recently, we have shown that aquometmyoglobin, which has an Fe<sup>3+</sup> heme with a water molecule at the sixth coordination, can be photoreduced at 80 K, yielding a myoglobin with a photodissociable water ligand bound to the ferrous heme iron (Fe<sup>2+</sup>). We have investigated the rebinding of the water ligand after laser flash excitation using transient absorption spectroscopy with monitoring in the Soret band from 12 to 150 K and 10 ns to 10 s. The kinetics are non-exponential, owing to the heterogeneous nature of the protein ensemble investigated, and are described with a kinetic model involving an enthalpy barrier distribution. Above 50 K, the temperature dependence of the kinetics follows the Arrhenius law, implying that ligand rebinding occurs by classical barrier crossing. Below 50 K, the rebinding occurs markedly faster than predicted from the Arrhenius law, suggestive of molecular tunneling through the barrier. We have used a simple model to describe the kinetics, and fitting of this model to the experimental data allowed us to determine the model parameters governing the tunneling rate coefficient. Copyright © 2000 John Wiley & Sons, Ltd.

**KEYWORDS:** ligand binding; kinetics; thermal activation; molecular tunneling; myoglobin

## INTRODUCTION

Transition state theory (TST) is most commonly used to describe chemical reaction rates. Reactant molecules are treated as an ensemble of classical particles vibrating in the reactant well, having a Boltzmann distribution of energies. They turn into product molecules by overcoming an energy barrier, the highest point of which specifies the transition state. Classically, only reactants with energies equal to or larger than the transition state energy are able to surmount the barrier. There exists, however, another mechanism by which chemical reactions can occur that involves quantum-mechanical tunneling through the barrier.<sup>1,2</sup> This phenomenon is based on the particle-wave duality of matter, which implies a non-zero probability of finding a particle under the barrier, thus having a net negative energy. The tunnel effect is relevant for systems with small mass so that the de-Broglie wavelength may become comparable to the barrier width. Indeed, electron-transfer reactions are described by Marcus theory in terms of an electron

tunneling mechanism.<sup>3</sup> The relevance of tunneling for biological reactions has been known for a long time.<sup>4</sup> In recent years, tunneling has been implied in enzymatic catalysis of hydrogen-transfer reactions.<sup>5</sup> Even entire molecules can tunnel through a reaction barrier.<sup>6</sup> A prime example of molecular tunneling occurs in the rebinding of carbon monoxide (CO) to the Fe<sup>2+</sup>–protoporphyrin-IX prosthetic group in heme proteins after photodissociation below 50 K.<sup>7</sup>

In this paper, we present a study of the tunnel effect of water ligands in myoglobin, a small heme protein. In aquometmyoglobin, the heme iron is in the Fe<sup>3+</sup> state and a water ligand is bound at the sixth coordination, the ligand binding site. The iron can be photoreduced<sup>8,9</sup> and at temperatures below 150 K an intermediate state forms<sup>10,11</sup> where the water ligand is bound to the reduced heme iron (Fe<sup>2+</sup>) in a photolyzable complex.<sup>12</sup> A water ligand is particularly convenient for studying tunneling, since the isotope effect can easily be observed by replacing the H<sub>2</sub>O solvent with D<sub>2</sub>O. Using time-resolved spectroscopy, we have measured ligand binding after photodissociation from 10 ns to 10 s for temperatures between 12 and 150 K. We observed that the kinetics below 50 K are much faster than predicted from the Arrhenius law and can be explained by quantum-

\*Correspondence to: G. U. Nienhaus, Department of Biophysics, University of Ulm, D-89069 Ulm, Germany.

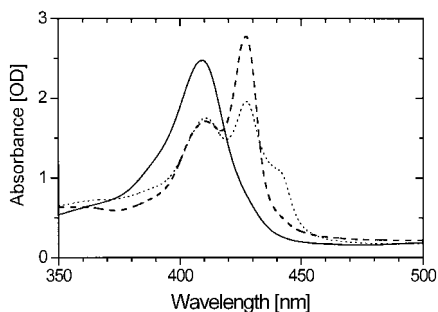


**Figure 1.** Absorption spectrum of aquometmyoglobin ( $\text{Fe}^{3+}$  with  $\text{H}_2\text{O}$  ligand) at room temperature (solid line) and partially reduced sample before (dashed line) and after (dotted line) illumination with white light for 5 min at 12 K.

mechanical tunneling. A simple model, introduced by Frauenfelder,<sup>13</sup> was used to describe the data and to extract model parameters governing the kinetics.

## EXPERIMENTAL

Freeze-dried sperm whale myoglobin (Mb) was purchased from Sigma (St Louis, MO, USA) and dissolved in 75% glycerol–25% 200 mM potassium phosphate buffer, pH 6.6. The final protein concentration was 10 mM. The sample was centrifuged at 16000 g at room temperature for 8 min. Approximately 2  $\mu\text{l}$  of the solution were sandwiched between a microscope coverslip and an optical window which were separated by a 15  $\mu\text{m}$  thick Mylar spacer that defines the sample thickness. The room temperature spectrum of the metmyoglobin sample in the visible region shows a strong absorption at 410 nm, the Soret band, which arises from a  $\pi$ – $\pi^*$  transition of the heme group (Fig. 1, solid line). The sample was subsequently loaded in a closed-cycle refrigerator (CTI Cryogenics, SC & M22CP). The sample temperature was measured with a silicon diode sensor and kept at the desired value with a digital temperature controller (Lakeshore, DRC 93C). The cryostat had four windows, two of which (along one axis) were made of Mylar and the other two (along the perpendicular axis) of glass. The sample was mounted at 45° with respect to the cryostat windows so that it could be irradiated with x-rays and also photodissociated through the Mylar windows, whereas the absorption changes were monitored through the glass windows.

After cooling the sample to 80 K, it was irradiated for 48 h with polychromatic x-rays from a copper anode running at 40 kV and 30 mA. Color centers generated from this procedure were removed by warming the sample to 140 K for 10 min. Approximately 50% of the protein molecules were reduced during the irradiation. The narrow spectra of the irradiated sample in Fig. 1 indicate that radiation damage is insignificant at 80 K even after x-ray exposure for 48 h. The spectrum of the

partially reduced sample at 12 K (dashed line in Fig. 1) shows the characteristic absorption of the intermediate state  $\text{Mb}^*\text{H}_2\text{O}$  at 428 nm.<sup>10–12</sup> Upon illumination with white light at 12 K, this line decreases, and a new Soret band appears at  $\sim 437$  nm, near the maximum absorption of (unligated) deoxymyoglobin. Moreover, a charge-transfer band at 770 nm is observable after photolysis,<sup>10</sup> verifying the presence of a high-spin unligated  $\text{Fe}^{2+}$  heme iron.

The rebinding kinetics were monitored using a transient absorption spectrometer. The sample was photolyzed with an 80 mJ, 6 ns pulse of a frequency-doubled Nd:YAG laser (Continuum, NY61). The change in absorption was monitored at 440 nm using an incandescent lamp and monochromator (Instruments SA, H10 1200VIS) for the monitoring illumination and an additional monochromator (Instruments SA, H10 800VIS), filters and photomultiplier tube (PMT) (Hamamatsu, R5600U) for detection. The PMT output was amplified and recorded with a digital oscilloscope (Tektronix, TDS 520) for the fast time-scales (10 ns to 100  $\mu\text{s}$ ) and a laboratory-built digitizer with a logarithmic time base for the slower time-scales (1  $\mu\text{s}$  to 10 s). The rebinding kinetics were measured from 12 to 150 K.

## RESULTS AND DISCUSSION

Below 160 K in 75% (v/v) glycerol–buffer, it has been well established that global protein motions are frozen out, and the ligands cannot escape from the heme pocket, an internal cavity in ligand-binding heme proteins, after photodissociation.<sup>14,15</sup> The kinetics of ligand recombination after photolysis can be described with a simple two-state model, where rebinding can occur via two mechanisms, (1) thermally activated crossing over an enthalpy barrier of height  $H$  and (2) quantum-mechanical tunneling through the barrier. The rate coefficient for the first mechanism is given by the Arrhenius relation:

$$k_A(H, T) = A_A \frac{T}{T_0} \exp\left(-\frac{H}{RT}\right) \quad (1)$$

where  $A_A$  is the (Arrhenius) pre-exponential factor,  $T$  is the absolute temperature,  $T_0$  is set to 100 K and  $R$  is the universal gas constant. In the simplest fashion, the rate coefficient for molecular tunneling can be parameterized by the Gamov expression:<sup>7,13</sup>

$$k_T = A_T(T) \exp\left\{-\frac{\gamma}{\hbar} [2M(H - E)]^{1/2} d\right\} \quad (2)$$

with tunneling prefactor  $A_T(T)$ ,  $\gamma$  being a geometric factor of order unity,  $\hbar$  Planck's constant,  $M$  tunneling mass and  $H - E$  the energy deficit of the particle under the barrier. In accordance with Ref. 13, we take the prefactor  $A_T(T)$  to be the only temperature-dependent term in the expres-

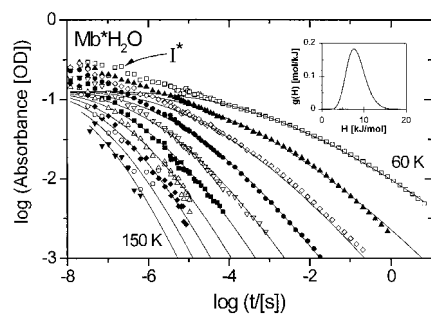


**Figure 2.** Rebinding kinetics of Mb\*H<sub>2</sub>O from 60 to 150 K, showing a fast (I\*) and slow component. Symbols, experimental data; lines, fit of the slower kinetic component with the Arrhenius law and a distribution of enthalpy barriers (shown in the inset) according to Eqns ((2)–(4))

sion, lumping together the attempt frequency and the phonon coupling.

### Arrhenius regime

To analyze the influence of molecular tunneling on the rebinding, it was necessary first to determine the parameters that govern rebinding in the region of classical barrier crossing. In Fig. 2, we show the rebinding kinetics of Mb\*H<sub>2</sub>O from 60 to 150 K. Two processes are observable, a fast process, labeled I\*, that is observed from 10 ns to 10 μs, and a slower one following I\* on the longer time-scales. Both processes are non-exponential in time. The fraction of proteins that rebind through I\* increases with temperature up to about 60 K, and their rebinding rates speed up with increasing temperature. This fast process is not relevant for the tunneling process we are investigating and we do not consider it here in more detail, but only note that similar fast processes have also been observed in dioxygen binding to myoglobin<sup>16</sup> and in other heme proteins.<sup>17</sup>

Frauenfelder and co-workers have shown that the non-exponential kinetics of the slow process can be explained by a classical, thermally activated barrier crossing, involving a heterogeneous ensemble of protein molecules in different conformational substates with similar overall structure but markedly different rebinding barriers.<sup>18</sup> With respect to ligand recombination, the ensemble is characterized by an enthalpy barrier distribution,  $g(H)$ , which is taken as independent of temperature (below 150 K) and gives the probability that a protein molecule has an enthalpy barrier between  $H$  and  $H + dH$ . Then, the fraction of proteins that have not rebound a ligand at time  $t$  after the photolysis pulse is given by

$$N(t) = \int dH g(H) \exp[-k_A(H, T)t] \quad (3)$$

The solid lines in Fig. 2 are fits of Eqn. (3) to the

rebinding kinetics of Mb\*H<sub>2</sub>O. We modeled  $g(H)$  as a gamma distribution:

$$g(H) = \text{constant} \times (H - H_{\min})^{\frac{(H_{\text{pk}} - H_{\min})}{\delta}} \times \exp\left[-\frac{(H - H_{\min})}{\delta}\right] \quad (4)$$

where the peak position  $H_{\text{pk}} = 7.7 \text{ kJ mol}^{-1}$ , minimum barrier  $H_{\min} = 0$ , width parameter  $\delta = 0.6 \text{ kJ mol}^{-1}$  and pre-exponential factor  $A_A = 1.6 \times 10^{10} \text{ s}^{-1}$  were obtained from the fit. The distribution is plotted in the inset of Fig. 2. Data points where rebinding from I\* was visible were not included during the fitting procedure. We note that the  $g(H)$  parameters given here differ from those reported earlier,<sup>11</sup> presumably because of the different photo-reduction technique applied.

### Tunneling regime

The excellent agreement between kinetic data and model [Eqns (1), (3) and (4)] above 50 K does not extend to the lower temperatures. The kinetics between 12 and 30 K (Fig. 3, top panel) are markedly faster than would be expected from the spectrum of barriers determined above 50 K and the Arrhenius relation. This is exemplified in the lower panel of Fig. 3, which compares the experimental data at 15 K with the kinetics calculated from the Arrhenius relation. Obviously, quantum-mechanical

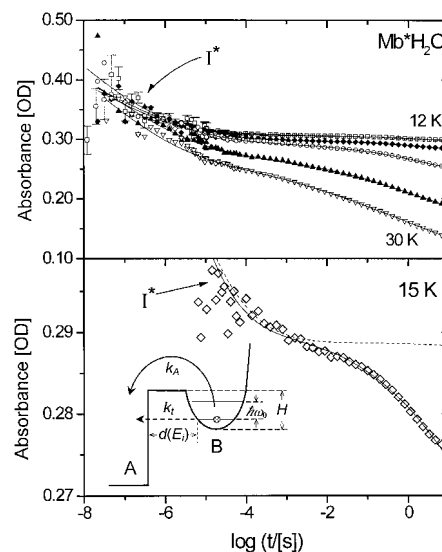


**Figure 3.** Top: rebinding kinetics of Mb\*H<sub>2</sub>O at 12, 15, 20, 25, and 30 K. Symbols, experimental data, with error bars shown only for the 12 K trace; solid lines, fits using the tunneling model (shown schematically in the inset) described in the text. Bottom: An expanded plot of the rebinding kinetics of Mb\*H<sub>2</sub>O at 15 K. Symbols, experimental data; solid line, fit using the tunneling model described in the text; dashed line, fit using the Arrhenius law

tunneling plays a significant role in the rate of ligand recombination. To determine the relevant tunneling parameters, we used a simple model proposed by Frauenfelder to describe the temperature dependence of tunneling of CO in myoglobin.<sup>13</sup> A schematic diagram of the model is shown in the inset of the lower panel of Fig. 3. The state from which recombination occurs, the photodissociated state (well B), is approximated by a harmonic potential, leading to energy levels,  $E_i$ , that are evenly spaced. The shape of the potential is governed by the frequency,  $\omega_0$ , which is taken as a fit parameter. The mass of the tunneling particle is assumed to be the reduced mass of the heme iron and the ligand. To recombine, the system has to move through the barrier into the ligand-bound state, denoted by A. At  $T > 0$ , tunneling will not only occur from the lowest level in well B, but also from the higher levels of the vibrational manifold, with a probability given by Boltzmann statistics. The total tunneling rate coefficient is thus given by

$$k_T(H, T) = \sum_i k_T(E_i, H, T) \times \exp[-E_i/(RT)] / \sum_i \exp[-E_i/(RT)] \quad (5)$$

where  $k_T(E_i, H, T)$  was calculated by integrating the action along the tunneling path at each energy level  $E_i$  for the barrier shape depicted in Fig. 3 (inset). The spatial separation between the two wells was assumed to depend linearly on the height of the barrier  $H$ , and therefore  $d(H) = d_0 H/H_{pk}$ , where  $d_0$  was treated as a free parameter in the fit.

From 12 to 30 K, kinetics were calculated by essentially using Eqn. (3). The rebinding rate coefficient was, however, taken to be the sum of the Arrhenius and tunneling rate coefficient. The tunneling parameters were determined by least-squares fitting of the model to the rebinding kinetics at each temperature with the  $g(H)$  parameters fixed to the values determined at the higher temperatures. The fast rebinding I\* component was included empirically by fitting the early times to a stretched exponential function,  $N_{I^*}(t) = N_{I^*}(0) \exp(-kt)^\beta$ . The solid lines in Fig. 3 represent the kinetics calculated with the described model, using the best-fit parameters; they are in excellent agreement with the data.

The temperature dependences of the prefactor  $A_T(T)$  and the tunneling distance  $d_0$  are shown in Fig. 4. Although the temperature dependence due to tunneling from vibrationally excited states is included in the model, the prefactor nevertheless changes (increases) with temperature. This suggests that the phonon involvement in the tunneling is not taken into account properly by this simple model. The temperature dependence of  $A_T(T)$  is a

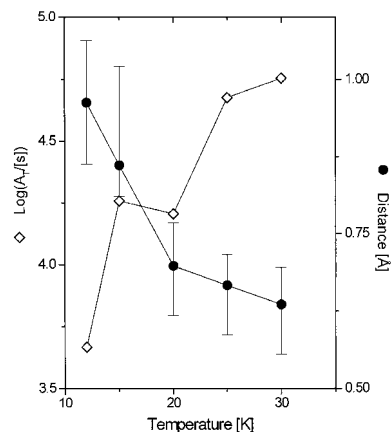


**Figure 4.** Temperature dependence of the tunneling prefactor  $A_T$  and tunneling distance  $d_0$  from the fits with the tunneling model. The error bars represent the 68% confidence level in  $d_0$ . The accuracy of  $A_T$  is not well determined because of the interdependence between  $A_T$ ,  $d_0$  and  $\omega_0$

consequence of the model chosen, in particular the barrier shape (Fig. 3, inset), and therefore not very meaningful. In a more elaborate model involving two bound states, the temperature dependence of the tunneling would be governed by the overlap of the vibrational wavefunctions, i.e. the Franck–Condon factor.<sup>4,6</sup>

For the tunneling distance  $d_0$ , the fit yielded values around 1 Å, similar to the 1.2 Å obtained for CO tunneling in MbCO.<sup>13</sup> The low-temperature x-ray structure of photodissociated MbCO shows that the CO ligand moves by several ångströms upon binding.<sup>15</sup> Note that this shift does not reflect the barrier width, but is merely an upper limit. Assuming also a well-defined binding site of the water ligand in the heme pocket for our system, one would have expected the barrier width  $d_0$  to remain fairly constant. However, a global fit of the data in Fig. 3 could only be achieved by allowing this parameter to vary somewhat around 1 Å.

From the fit, we also obtained the vibrational level spacing  $\omega_0$  in well B. It decreased from 450  $\text{cm}^{-1}$  at 12 K to 90  $\text{cm}^{-1}$  at 30 K (data not shown). These values appear reasonable as they are in the range of low-frequency modes of the Fe–protoporphyrin-IX molecule, which have been implicated in the bond formation process.<sup>19</sup>

To summarize, the extremely simple kinetic model applied here yielded tunneling parameters in a physically reasonable range. Their temperature dependences, however, indicate deficiencies of the model. Finally, we mention that preliminary data have been obtained on ligand recombination using Mb\*D<sub>2</sub>O. A significant difference in the rebinding kinetics of Mb\*D<sub>2</sub>O compared with Mb\*H<sub>2</sub>O was observed, providing additional evidence that tunneling is playing a significant role in the rebinding kinetics at these temperatures. The observed tunnel effect was much larger than we expected from the

change in reduced mass of the iron–ligand system. This result warrants further investigation.

## CONCLUSIONS

Quantum-mechanical tunneling has been observed in the ligand rebinding kinetics of Mb\*H<sub>2</sub>O below 60 K. With a simple model,<sup>13</sup> it was possible to obtain a very good description of the kinetic data, and the fit yielded the approximate tunneling distance, attempt frequency and the energy level spacing in the reactant well. Although these parameters were in a reasonable range, their temperature dependences point to deficiencies of the model. Note that the tunneling system was treated as a free particle after barrier penetration, as in nuclear  $\alpha$ -decay. In a more elaborate model, we will describe the reaction as an electron–nuclear tunneling transition between two harmonic wells.

## Acknowledgements

D. C. Lamb thanks the University of Ulm for travel support. This work was written while G. U. Nienhaus was on sabbatical leave at Stanford University, supported by the Stiftung Volkswagenwerk. The support of the Graduiertenkolleg 328 is also gratefully acknowledged.

## REFERENCES

1. Goldanskii VI, Trakhtenberg LI, Fleurov VN. *Tunneling Phenomena in Chemical Physics*. Gordon and Breach: New York, 1989.
2. Bell RP. *The Tunneling Effect in Chemistry*. Chapman and Hall: New York, 1980.
3. Marcus RA, Sutin N. *Biochem. Biophys. Acta* 1985; **811**: 265–322.
4. Chance B, DeVault DC, Frauenfelder H, Marcus RA, Schrieffer JR, Sutin N. (eds). *Tunneling in Biological Systems*. Academic Press: New York, 1979.
5. Kohen A, Klinman JP. *Acc. Chem. Res.* 1998; **31**: 397–404.
6. Goldanskii VI. *Nature (London)* 1976; **279**: 109–115.
7. Alben JO, Beece D, Bowne SF, Eisenstein L, Frauenfelder H, Good D, Marden MC, Moh PP, Reinisch L, Reynolds AH, Yue KT. *Phys. Rev. Lett.* 1980; **44**: 1157–1160.
8. Blumenfeld L. *Problems of Biological Physics*. Springer: Berlin, 1981.
9. Prusakov VE, Steyer J, Parak FG. *Biophys. J.* 1995; **68**: 2524–2530.
10. Lamb DC, Ostermann A, Prusakov V, Parak FG. *Eur. Biophys. J.* 1998; **27**: 113–125.
11. Lamb DC, Prusakov V, Engler N, Ostermann A, Schellenberg P, Parak FG, Nienhaus GU. *J. Am. Chem. Soc.* 1998; **120**: 2981–2982.
12. Engler N, Ostermann A, Gassmann A, Lamb DC, Prusakov VE, Schott J, Schweitzer-Stenner R, Parak FG. *Biophys. J.* **78**: 2081–2092.
13. Frauenfelder H. In *Tunneling in Biological Systems*, Chance B, DeVault DC, Frauenfelder H, Marcus RA, Schrieffer JR, Sutin N, (eds). Academic Press: New York, 1979; 627–649.
14. Nienhaus GU, Young RD. In *Encyclopedia of Applied Physics*, vol. 15, Trigg G, (ed). VCH; New York, 1996; 163–184.
15. Schlichting I, Berendzen J, Phillips GN Jr., Sweet RM. *Nature (London)* 1994; **371**: 808–812.
16. Jongeward KA, Magde D, Taube DJ, Marsters JC, Traylor TG, Sharma VS. *J. Am. Chem. Soc.* 1988; **110**: 380–387.
17. Doster W, Bowne SF, Frauenfelder H, Reinisch L, Shyamsunder E. *J. Mol. Biol.* 1987; **194**: 299–312.
18. Austin RH, Beeson KW, Eisenstein L, Frauenfelder H, Gunsalus IC. *Biochemistry* 1975; **14**: 5355–5373.
19. Zhu L, Widom A, Champion PM. *J. Phys. Chem.* 1997; **107**: 2859–2871.